ELSEVIER

Biophysical Chemistry 60 (1996) 99–110

Biophysical Chemistry

Simulation of voltage-dependent interactions of α-helical peptides with lipid bilayers

P.C. Biggin, M.S.P. Sansom *

Laboratory of Molecular Biophysics, University of Oxford, Rex Richards Building, South Parks Road, Oxford OX1 3QU, UK

Received 30 October 1995; revised 30 January 1996; accepted 31 January 1996

Abstract

Pore formation in lipid bilayers by channel-forming peptides and toxins is thought to follow voltage-dependent insertion of amphipathic α-helices into lipid bilayers. We have developed an approximate potential for use within the CHARMm molecular mechanics program which enables one to simulate voltage-dependent interaction of such helices with a lipid bilayer. Two classes of helical peptides which interact with lipid bilayers have been studied: (a) δ-toxin, a 26 residue channel-forming peptide from *Staphylococcus aureus*; and (b) synthetic peptides corresponding to the $\alpha 5$ and $\alpha 7$ helices of the pore-forming domain of *Bacillus thuringiensis* CryIIIA δ-endotoxin. Analysis of δ-toxin molecular dynamics (MD) simulations suggested that the presence of a transbilayer voltage stabilized the inserted location of δ-toxin helices, but did not cause insertion per se. A series of simulations for the $\alpha 5$ and $\alpha 7$ peptides revealed dynamic switching of the $\alpha 5$ helix between a membrane-associated and a membrane-inserted state in response to a transbilayer voltage. In contrast the $\alpha 7$ helix did not exhibit such switching but instead retained a membrane associated state. These results are in agreement with recent experimental studies of the interactions of synthetic $\alpha 5$ and $\alpha 7$ peptides with lipid bilayers.

Keywords: δ-Toxin; δ-Endotoxin; Channel-forming peptide; Molecular dynamics; Transbilayer potential

1. Introduction

Many channel-forming peptides (CFPs; e.g. melittin, alamethicin, δ-toxin [1]) and membrane-active toxins (e.g. colicins, δ-endotoxin [2]) interact with lipid bilayers in a voltage-dependent fashion. The structures adopted by several such peptides and toxins when in an aqueous environment have been determined [3]. The properties of the channels formed when these molecules interact with lipid bilayers and cell membranes have been characterised. However, rather less is understood of the mechanisms of their interaction with lipid bilayers [4] and of how such interactions are promoted by the presence of a transbilayer voltage difference. The difficulties of direct structural investigations of transient voltage-induced events lead us to adopt a simulation-based approach to investigating possible mechanisms of peptide-bilayer interactions.

δ-Toxin is a 26 residue peptide produced by *Staphylococcus aureus* [5]. At concentrations lower than 2 μM δ-toxin forms weakly cation selective ion channels in planar lipid bilayers [6]. At higher concentrations (> 2 μM) δ-toxin induces lysis of cells [7] and also of synthetic vesicles [8]. However,

* Corresponding author. Tel.: +44-1865-275371; fax: +44-1865-275182; e-mail: mark@biop.ox.ac.uk.

PII S0301-4622(96)00015-4

recent studies of synthetic δ-toxin analogues suggest that channel formation and membrane lysis are independent events [9]. NMR and other spectroscopic studies of the conformation of δ-toxin reveal that it forms an amphipathic α-helix The δ-toxin sequence is:

fM-A-Q-D-I-I-S-T-I-G-D-L-V-K-W-I-I-D-T-V-N-K-F-T-K-K

where fM indicates formyl-methionine. Thus at neutral pH the net charge of the peptide is expected to be zero. Channel formation by δ-toxin requires the presence of a transbilayer voltage difference [6]. As for many such CFPs this has been interpreted in terms of voltage-dependent insertion of δ-toxin helices into a bilayer coupled with self-assembly of parallel helix bundles to generate transbilayer pores [10].

The δ-endotoxins are a group of membrane toxins that exert their toxic effect by the formation of pores [11,12] in the epithelial cell membranes of various target insects. The structure adopted by δ-endotoxin CryIIIA in aqueous solution has been determined by X-ray diffraction to a resolution of 2.5 Å [13]. The toxin is comprised of three domains. The first domain is the pore-forming domain. It is made up of bundle of 6 α-helices surrounding a central α-helix, α5. Significantly, the sequence of the α5 helix is highly conserved throughout the δ-endotoxin family [13]. It has been suggested that α5 may play a key role in membrane insertion and channel formation. In particular, the α5 helix is amphipathic (a common feature of CFPs) and mutations of the toxin sequence in this region affect the toxic activity of the protein [14,15].

A possible model for ion channel formation by δ-endotoxin involves insertion of the α5 helix into a membrane [16]. It has been shown that a peptide corresponding to the α5 helix will insert into and self-associate within a membrane [17]. Furthermore, synthetic α5 peptide forms ion channels in lipid bilayers in a voltage-dependent manner [16]. In contrast, a peptide corresponding to α7 does not insert or self-associate but instead adopts a membrane-associated state on the bilayer surface. These two peptides:

α5: F-L-T-T-Y-A-Q-A-A-N-T-H-L-F-L-L-K-D-A-Q-I-Y-G

α7: Y-E-S-W-V-N-F-N-R-Y-R-R-E-M-T-L-T-V-L-D-L-I-A-L-F

thus provide a good model system for investigating contrasting modes of helical peptides with lipid bilayers.

In this paper we describe MD simulations on δ-toxin and on α5 and α7 helices in which approximate terms representing the hydrophobic core of a lipid bilayer and a transbilayer voltage are included in the potential energy function. Such simulations suggest plausible models for the effects of a transbilayer voltage difference on the interactions of α-helical peptides with lipid bilayers. Our results are in agreement with available experimental data, suggesting that simulations may aid the formulation of molecular mechanisms for pore formation by CFPs and by more complex toxins.

2. Methods

All simulations were performed using CHARMm V23.3 run on a DEC 3000 400 workstation or a Silicon Graphics (Mountain View, CA, USA) Indigo R3000 workstation. Molecular modelling and viewing was performed using Quanta V4.1.1 (Molecular Simulations). All auxiliary programs were written in Fortran 77.

2.1. Additions to the charmm potential energy function

MD simulations and potential energy calculations were performed using the Charmm V23.3 potential energy function (E_{CHARMM}), modified to include terms representing: (a) the interactions of the sidechains of an α-helical peptide with the hydrophobic core of a lipid bilayer (E_{BIL}); and (b) a difference in voltage between the two faces of the lipid bilayer ($E_{\Delta V}$). Thus,

$$E = E_{\mathrm{CHARMM}} + E_{\mathrm{BIL}} + E_{\Delta V}$$

The bilayer core was modelled as a hydrophobic continuum spanning from $z = -d$ to $z = +d$ (where

Table 1
Hydrophobicity scale for E_{BIL}

Residue	H_i (kcal/mol)
F	−3.09
L	−2.97
I	−2.97
W	−2.81
V	−2.33
C	−2.05
M	1.92
A	−0.82
P	−0.60
T	−0.57
G	−0.55
S	−0.05
H	+1.54
Y	+1.63
D	+1.82
Q	+2.27
K	+2.31
E	+2.53
N	+2.62
R	+3.64
Terminus [a]	+4.10

For each residue, the change in free energy on transfer from an interfacial to a bilayer location is listed, using the values from Ref. [21].

[a] This term reflects the energetic cost of transfer of the potential H-bonding groups at the terminus of an α-helix.

z is the bilayer normal axis and $2d$ is the bilayer thickness). This approximation is similar to those used by e.g. Edholm and Jähnig [18] in MD studies of bilayer-spanning peptides and by Milik et al. [19] in Monte Carlo simulations of peptide/bilayer interactions. A hydrophobicity index, H_i, is applied to the sidechain of each residue, and to the two exposed termini of the helix (see Table 1). The potential energy of a residue is a function of the z-coordinate of the geometric centre of its sidechain ($f(z_i)$). Thus the peptide/bilayer interaction energy is given by:

$$E_{BIL} = \sum_i H_i f(z_i)$$

where summation is over the residues of the helix, where $z = 0$ corresponds to the centre of the bilayer, and where

$$\begin{aligned} f(z) &= 1 \quad \text{if } |z| \ll d \\ f(z) &= 0 \quad \text{if } |z| \gg d \end{aligned} \tag{3}$$

Thus, for a residue i the bilayer energy is H_i within the bilayer ($|z| < d$), is zero outside the bilayer ($|z| \gg d$), and varies smoothly (see Appendix) in the 'interfacial' region ($|z|$ ca. d).

A problem arises in selecting an appropriate hydrophobicity scale (H_i) — over 40 such scales have been described [20]. We have elected to use the scale which was previously employed in Monte Carlo simulations of the interaction of simplified models of peptides with a bilayer [21,22]. This scale (Table 1) is derived from that of Roseman [23] and takes into account two important factors: (a) amino acids are assumed to be in a helical conformation; and (b) prior to bilayer insertions the helix occupies an interfacial location. These are important considerations with in the context of our simulations in which we assume that: (a) the peptides are α-helical; and (b) the helices are present at the bilayer interface before insertion proceeds. In preliminary calculations we have considered possible alternative hydrophobicity scales, e.g. that of Engelman et al. [24]. Although these scales yield different absolute values of E_{BIL}, the energy maps (see below) for rotation of a peptide helix relative to the bilayer were qualitatively similar to those of the H_i scale adopted.

To include a transbilayer voltage difference (ΔV) in the simulations an additional term ($E_{\Delta V}$) was incorporated into Charmm. The *trans* face of the bilayer ($z < -d$; where $2d = 30$ Å is the bilayer thickness) was set to $V = 0$ mV, whereas the *cis* face of the bilayer ($z > +d$) was set to $V = \Delta V$, e.g. $V = +100$ mV). The voltage was varied linearly across the bilayer region ($-d < z < +d$) such that an atom j with partial charge q_j and z-coordinate z_j was subjected to a potential:

$$E_{\Delta V} = \frac{q_j F \Delta V (z_j + d)}{2d}, \tag{4}$$

where F is Faraday's constant. As it stands this potential is not differentiable at the water/bilayer 'interface' ($|z| = d$). A simple smoothing factor was applied in order to remedy this (see Appendix).

2.2. Molecular dynamics simulations

Initial models of the helices were generated by restrained MD simulations and simulated annealing, as described in previous papers [25,26]. In all simulations an extended atom representation was employed,

whereby only those H atoms bonded to non-carbon atoms are represented explicitly. In the MD simulations per se the SHAKE algorithm was employed [27]. The timestep of the MD simulations was 0.5 fs and coordinate sets were saved every 1 ps for subsequent analysis. The heating phase was of 5 ps duration, during which the system was heated from 0 K to 300 K in 15 K, 0.25 ps steps. The equilibration phase was of 5 ps duration, during which the velocities were rescaled every 0.05 ps in order to maintain a temperature of 300 ± 10 K. The production phase of the MD runs was e.g. 500 ps duration, during which velocity rescaling was not applied.

3. Results

3.1. Possible helix orientation

Before discussing the simulations, it is helpful to consider possible orientations of a helix relative to the lipid bilayer. As we are concerned with insertion per se of membrane-active peptides into a bilayer, we do not consider the equilibrium of peptide helices between bulk solution and an interfacial location.

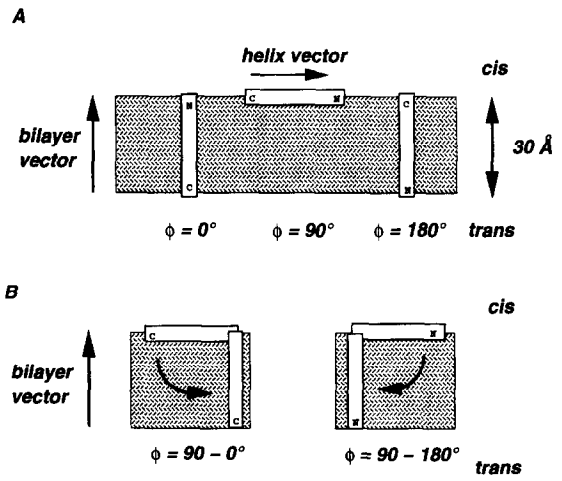

Fig. 1. Helix orientations. (A) shows the definition of the helix axis vector (from C to N terminus) and of the bilayer vector (from *trans* to *cis*). Three orientation of the helix are show: membrane associated ($\phi = 90°$), and two membrane inserted orientations ($\phi = 0°$; $\phi = 180°$). (B) shows the rotations performed during the energy 'mapping' procedure, from $\phi = 90° \rightarrow 0°$ and from $\phi = 90° \rightarrow 180°$.

Rather, we consider possible interactions of a helix already 'bound to' a bilayer, as illustrated in Fig. 1. This may be described, albeit approximately, by the z coordinate of the centre of mass of the helix (recalling that the z-axis is equivalent to the bilayer normal), and by the angle, ϕ, between the helix axis vector (running from the C-terminus to the N-terminus, i.e. parallel to the helix backbone dipole) and the z-axis. In this fashion we may define two extreme orientations of a membrane bound helix: (a) membrane-*associated*, for which $z \approx d$ and $\phi \approx \pm 90°$; and (b) membrane-*inserted*, for which $z \approx 0$ Å and $\phi \approx 0°$ or 180°. A number of spectroscopic studies on the interactions of peptides with oriented bilayers [28–30] suggest that peptides may adopt either a membrane-associated or a membrane-inserted state depending upon, inter alia, the peptide sequence, the peptide:lipid ratio, lipid phase and the magnitude and size of the transbilayer voltage. The results of the simulations are discussed in terms of helix orientation relative to the bilayer normal. This may be summarized by the helix order parameter, S, defined as:

$$S = \frac{(3\langle\cos^2\phi\rangle - 1)}{2} \tag{5}$$

where $\langle\cos^2\phi\rangle$ represents the time-averaged orientation of a helix with respect to the bilayer normal. For a helix in a membrane inserted position ($\phi \approx 0°$ or 180°) $S \approx 1$. Conversely for a helix in a membrane-associated state ($\phi \approx \pm 90°$) $S \approx -0.5$.

3.2. Energy maps

The potential energy of a helix as a function of its orientation may be explored by use of an 'energy mapping' procedure. This is intended to reveal the changes in potential energy as a helix is inserted into a bilayer (Fig. 1). Thus, a helix starts in a membrane-associated location ($\phi = 90°$, $z \approx +15$ Å). In this location the helix is first rotated about its long axis such that E_{BIL} is minimized. Thus, an amphipathic helix is oriented such that its hydrophobic face is directed towards the bilayer region, whilst its hydrophilic face is pointing away from the bilayer. The helix is then rotated such that either its C-terminus crosses the bilayer (by varying ϕ from 90° to 0°; see Fig. 1), or such that its N-terminus crosses

the bilayer (ϕ from 90° to 180°), and $E = E_{BIL} + E_{\Delta V}$ is evaluated. Such a map thus provides an indication of the energy barriers to insertion of a surface associated peptide helix. Note that during these calculations the transbilayer voltage (ΔV) may be set so that the face of the bilayer on which the peptide is present (defined as the *cis* face) is either at a *cis* positive or a *cis* negative voltage relative to the opposite (*trans*) face of the bilayer. In each of the following 'energy mapping' simulations a voltage difference of $\Delta V = +100$ mV, i.e. *cis* positive, was applied.

To test this procedure, helix/bilayer potential energy calculations were performed for an Ac-Ala_{20}-NH_2 α-helix. This helix is entirely hydrophobic and has a dipole moment along its axis of ca. 63D. An equipotential contour plot for the interaction of this helix with a bilayer in the presence of $\Delta V = +100$ mV is shown in Fig. 2. At first glance the energy surface defined by these contours is somewhat complex and difficult to follow. The interpretation of the peptide/bilayer interaction is somewhat clearer if one considers the trajectory of the helix defined by the 'energy mapping' rotation of the helix. This is shown in Fig. 2 by the thick solid line superimposed on the contour map. Moving along this trajectory, it is evident that the membrane associated state ($\phi = +90°$; $z = +d$) is less stable than the membrane inserted state ($z = +0$). This suggests that the nature of the peptide/bilayer interaction may be dissected if one considers the energy as a function of the rotation angle (ϕ) along this trajectory, as is the case in Fig. 3. The initial orientation of the helix used to generate the energy map (Fig. 3A) was membrane associated ($\phi = +90°$; $z = +d$). Comparing $\phi = 0°$ with $\phi = 180°$ reveals that N-terminal insertion (to $\phi = 180°$) is ca. 2 kcal/mol favourable relative to C-terminal insertion (to $\phi = 0°$), as expected for a 63D dipole reoriented with respect to a 100 mV/30 Å electrostatic field. For small perturbations around $\phi = 90°$ it can be seen that there is a small (ca. 1 kcal/mol) barrier resisting helix insertion into the bilayer. This reflects the energetic cost of loss of H-bonding at the helix termini upon their insertion. However, this is soon overcome by the favourable sidechain/bilayer interactions, thus stabilizing the inserted orientation by ca. −5 kcal/mol relative to the associated state.

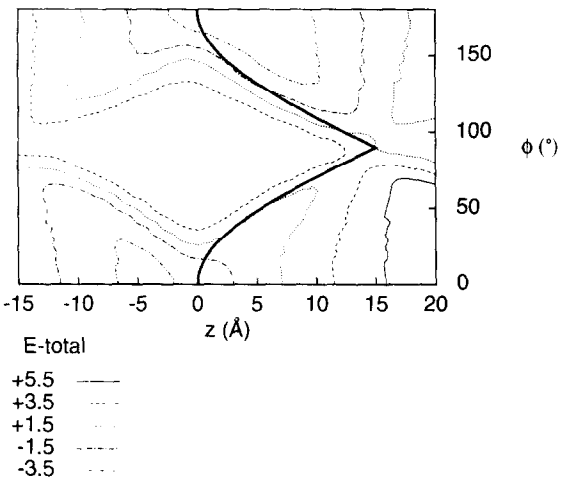

Fig. 2. Equipotential contour plot of the total peptide/bilayer interaction energy for an Ac-Ala_{20}-NH_2 helix. The thick solid line superimposed upon the contours corresponds to the (z, ϕ) trajectory for the helix rotation used to generate the corresponding energy map in Fig. 3A.

The energy map for the interaction of a δ-toxin helix with a bilayer (Fig. 3B) is, predictably, somewhat more complex. Overall, a single δ-toxin helix seems to favour a surface associated state, even in the presence of a transbilayer voltage difference. Indeed, the $E_{\Delta V}$ curve is quite complex, as result of the combined effect of the helix backbone dipole and of the disposition of anionic and cationic sidechains along the length of the helix. In addition to the global energy minimum corresponding to a bilayer associated δ-toxin helix, there are a local energy minima corresponding to both C-terminal inserted ($\phi = 0°$) and N-terminal inserted ($\phi \approx 160°$) helices. The relative energies of these two local minima are quite sensitive to the starting position on z of the helix during energy mapping. Thus, one would predict isolated δ-toxin helices to prefer a bilayer associated orientation, but possibly also to be capable of occupying metastable inserted orientations.

Comparison of the energy maps for the $\alpha 5$ and $\alpha 7$ helices (Fig. 3CD) reveals marked difference in their predicted interactions with a bilayer. The energy map for rotation of $\alpha 5$ starting from a membrane associated location ($\phi = 90°$, $z = +15$ Å; Fig. 3C) reveals that N-terminal insertion is favoured by ca. 6 kcal/mol relative to either surface association or C-terminal insertion of the peptide helix. Stabi-

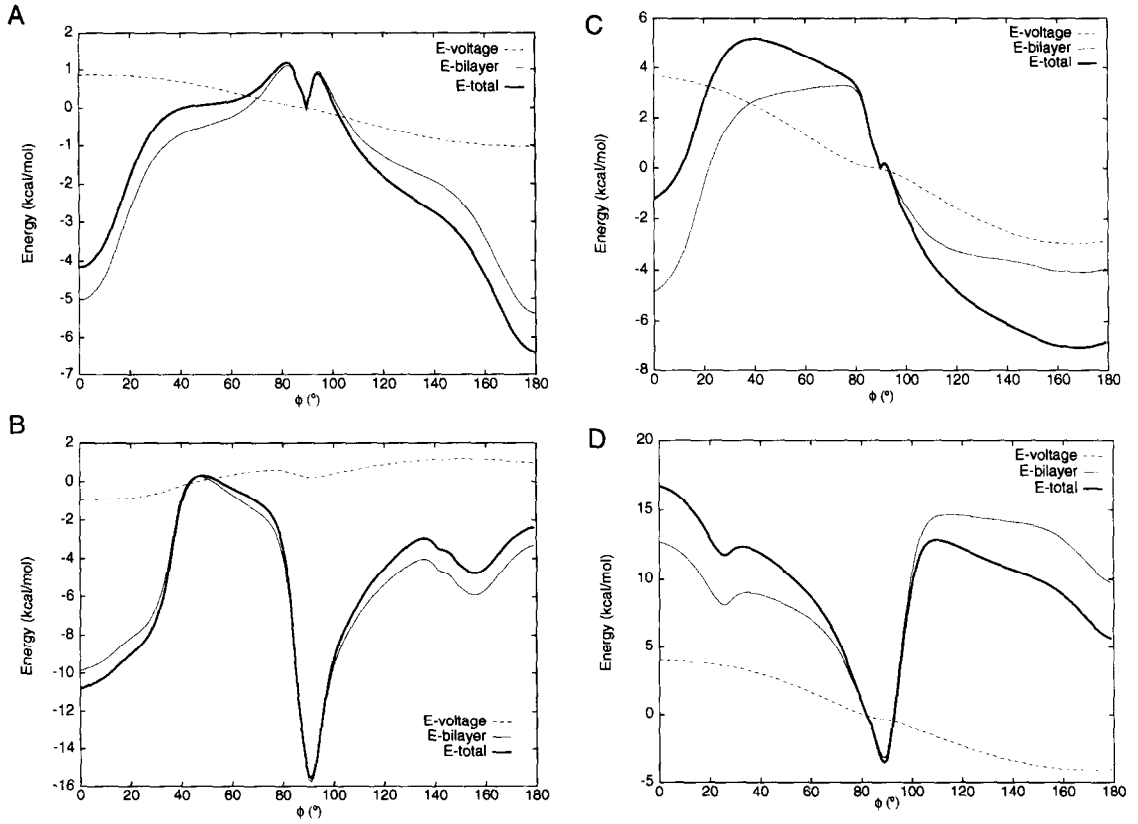

Fig. 3. Energy maps for helix rotations relative to the bilayer. In each figure the total peptide/bilayer energy ($E = E_{BIL} + E_{\Delta V}$; thick line) and its two components E_{BIL} (thin line) and $E_{\Delta V}$ (broken line) are shown, as the helix is rotated from a membrane associated ($\phi = 90°$) to a C-terminal inserted ($\phi = 0°$) or to an N-terminal inserted ($\phi = 180°$) orientation. In each map the total energy is normalized such that E is zero for the membrane associated ($\phi = 0°$) orientation. The maps shown are for: (A) Ac-Ala$_{20}$-NH$_2$; (B) δ-toxin; (C) α5; and (D) α7 helices.

lization of the N-terminal inserted ($\phi = 180°$) relative to the surface associated ($\phi = 90°$) state is due to $\Delta E_{\Delta V} \approx -3$ kcal/mol and $\Delta E_{BIL} \approx -4$ kcal/mol (for $\Delta V = +100$ mV). This preference for a membrane inserted state may be rationalized in terms of the sequence of α5. The N-terminus of the peptide is more hydrophobic than the C-terminus, thus favouring N-terminal insertion in terms of E_{BIL}. Furthermore, for $\Delta V > 0$, N-terminal insertion is favoured by the interaction of the helix dipole with the transbilayer electrostatic field.

The behaviour of α7 is different from that of α5. From the corresponding energy map (Fig. 3D), it may be seen that surface association ($\phi = 90°$) is favoured by ca. 10 kcal/mol relative to either inserted ($\phi = 0°$ or 180°) locations, regardless of the effect of $E_{\Delta V}$. This reflects the more polar nature of the α7 peptide. Thus α7 is predicted to be a surface-seeking peptide, unlike α5 which is predicted to be membrane-spanning. Both of these predictions are supported by recent experimental data [17,31].

3.3. Molecular dynamics simulations — δ-toxin

Energy mapping calculations (above) suggested that although the δ-toxin helix favours a membrane-associated orientation, a C-terminal inserted orientation ($\phi = 0°$) corresponds to a local energy minimum, stabilized by *cis* positive voltages. This has been explored in more detail by MD simulations of δ-toxins/bilayer interactions. Simulations in which a

Table 2
Helix order parameter in MD simulations

Initial orientation	ΔV (mV)	Duration (ps)	δ-Toxin	α5	α7
Associated	0	500	−0.47	+0.04	−0.37
Associated	+100	500	−0.47	+0.56	−0.42
Associated	+200	500	−0.47	+0.57	−0.46
Associated	0	0 to 250	−0.48	−0.19	−0.45
Associated	+100	250 to 500	−0.46	+0.74	−0.45
Associated	+200	250 to 500	−0.47	+0.65	-

The helix order parameter, $S = (3\langle\cos^2\phi\rangle - 1)/2$, is listed for the various MD simulations described. Note that for an ideal bilayer associated orientation $S = -0.5$ and $\phi = 90°$, whereas for an ideal inserted location $S = +1.0$ and $\phi = 0°$ or 180°.

δ-toxin helix was initially in a membrane associated orientation revealed that the peptide failed to insert, even if a transbilayer voltage of $\Delta V = +200$ mV was applied. Thus, for $\Delta V = 0$, +100 or +200 mV, $S = -0.47$ (Table 2, remembering that $S = +1$ for fully inserted, and −0.5 for an ideal membrane associated orientation). In simulations starting with an N-terminal inserted δ-toxin helix the helix generally remained in an inserted orientation, although in a simulation with $\Delta V = 0$ mV the helix reverted to a membrane associated orientation after ca. 200 ps. Such behaviour is consistent with the local nature of the minima in the energy map (Fig. 3B) which correspond to an inserted δ-toxin helix.

In addition to analyzing the rigid body movements of δ-toxin during these MD simulations, the conformation of the helix per se has been examined. Calculation of residue by residue (ϕ, ψ) variations over the course of the trajectories reveals that there is greater variation in the C-terminus of the helix than in the N-terminus. This is in broad agreement with NMR data obtained for δ-toxin in isotropic solution [32–35].

3.4. Molecular dynamics simulations — α5 and α7

MD simulations of the interactions of the two δ-endotoxin-derived peptides (α5 and α7) with the bilayer model confirmed the difference in their behaviour suggested by the energy map calculations. Consider first those simulations of α5 in which the helix starts in a membrane associated orientation (Table 2). In these simulations, S increases from +0.04 to +0.57 as the transbilayer voltage is increased from $\Delta V = 0$ to +200 mV. Thus, α5 has an inherent tendency to insert into the bilayer, but this is increased if a transbilayer voltage is imposed. If the MD simulations started with an α5 helix inserted into the bilayer, it remained inserted, with imposition

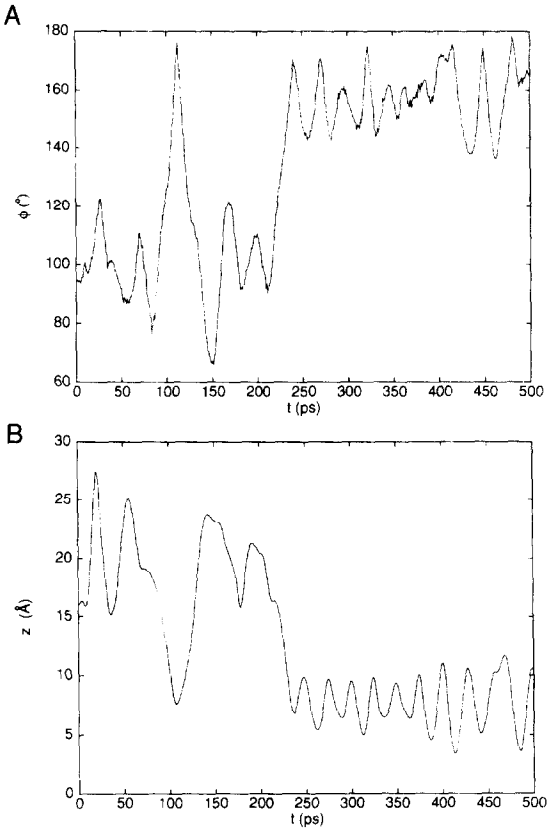

Fig. 4. MD simulations for α5. At $t = 0$ ps the helix is in a membrane associated orientation ($\phi = 90°$). For the first 250 ps, $\Delta V = 0$ mV. At $t = 250$ ps the transbilayer voltage is stepped to $\Delta V = +200$ mV, and remains at this value until the end of the simulation. (A) shows the trajectory for ϕ, the angle between the helix axis and the bilayer normal. (B) shows the trajectory of the z coordinate of the centre of the helix.

of a *cis*-positive voltage difference further stabilizing the inserted state. A further series of simulations explored the possibility of dynamic switching of an $\alpha 5$ helix between the associated and inserted orientations. Starting from an associated state, with no transbilayer voltage imposed, the $\alpha 5$ helix remains at the bilayer surface. At $t = 250$ ps the transbilayer voltage was increased to either $+100$ mV or $+200$ mV. As can be seen from the trajectories in Fig. 4, the stepwise imposition of a transbilayer voltage resulted in helix insertion. This is illustrated for $\Delta V = +200$ mV in Fig. 5, from which it can be seen that the N-terminus of the $\alpha 5$ helix inserts such that its C-terminus remains close to the interface. Conformational (residue by residue (ϕ, ψ)) analysis during this 'switched' trajectory revealed that at $\Delta V = 0$ mV the C-terminal segment (residues 14–21) of the

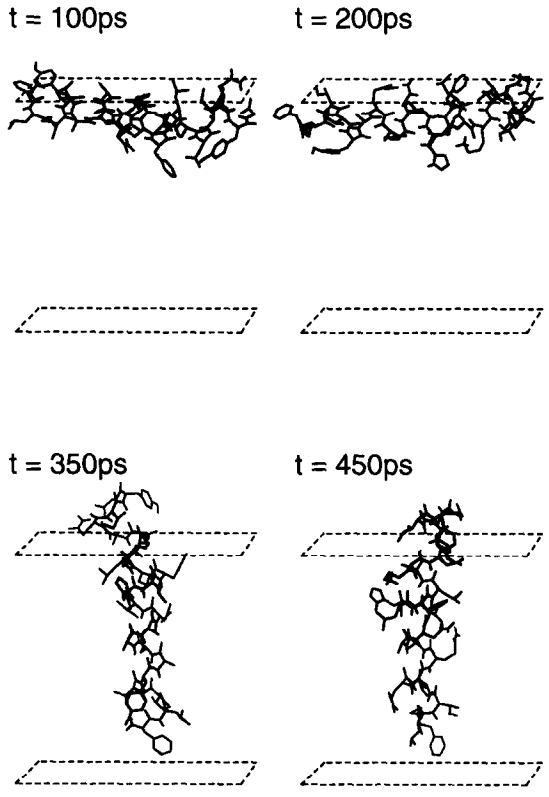

Fig. 5. Four snapshots of the $\alpha 5$ simulation in Fig. 3 (at $t = 100$, 200, 350 and 450 ps). For $t = 0$ to 250 ps, $\Delta V = 0$ mV; for $t = 250$ to 500 ps, $\Delta V = +200$ mV. The dotted planes indicate the extent of the bilayer, the upper plane at $z = +d$ and the lower plane at $z = -d$.

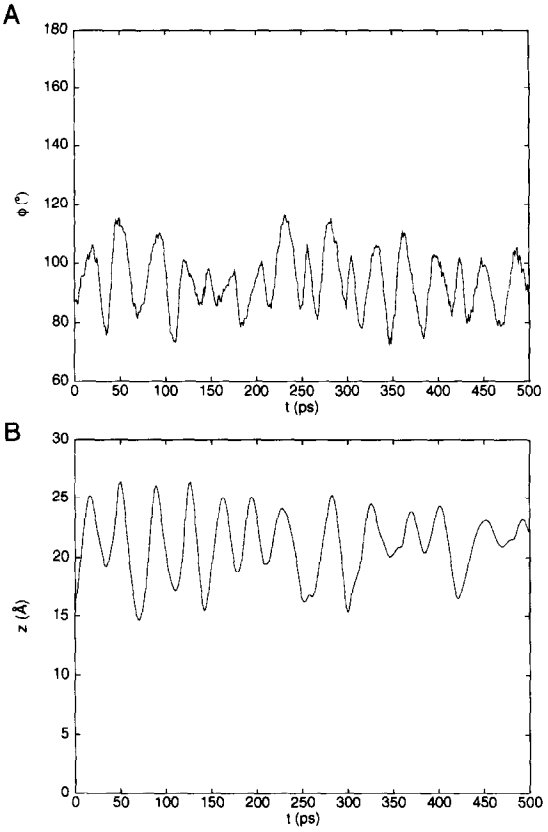

Fig. 6. MD simulations for $\alpha 7$. The simulation conditions were the same as in Fig. 3 for $\alpha 5$. At $t = 0$ ps the helix is in a membrane associated orientation ($\phi = 90°$). For the first 250 ps, $\Delta V = 0$ mV. At $t = 250$ ps the transbilayer voltage is stepped to $\Delta V = +200$ mV, and remains at this value until the end of the simulation. (A) shows the trajectory for ϕ, the angle between the helix axis and the bilayer normal. (B) shows the trajectory of the z coordinate of the centre of the helix.

$\alpha 5$ helix was more flexible than the N-terminal segment. Upon insertion, a reduction in C-terminal flexibility was seen.

The behaviour of $\alpha 7$ in MD simulations is in contrast with that of $\alpha 5$. Thus, in all simulations in which an $\alpha 7$ helix started in a membrane associated location it remained thus, with S ca. -0.4, regardless of whether or not either a constant or a 'switched' transbilayer voltage was applied (see Table 2 and Fig. 6). In simulations starting with $\alpha 7$ in an N-terminal inserted location, the helix tended to drift slowly back (on a 1000 ps timescale or thereabouts) to a membrane associated orientation. Overall, this is

consistent with the $\alpha 7$ energy map (Fig. 3D) which suggests that the global minimum is the associated orientation but that an N-terminal inserted helix might occupy a local minimum.

Overall, these MD simulations show that $\alpha 5$ has a tendency to insert into bilayers, increased by the presence of a *cis* positive transbilayer voltage difference. In contrast, $\alpha 7$ fails to insert, retaining a membrane associated location.

4. Discussion

4.1. Limitations of simulations

In the simulations described above a simple model of a hydrophobic bilayer core and of a transbilayer voltage difference are incorporated into the Charmm potential function. Before exploring the possible significance of the peptide/bilayer interactions observed it is important to consider possible limitations of these simulations. In particular, one should remember that the two potential terms added are approximations, and do not fully represent all the components of the real peptide/bilayer/water system.

The absence of explicit lipid molecules is expected to have two effects: (a) electrostatic interactions between the polar sidechains and lipid headgroups are ignored; and (b) the 'viscosity' of the bilayer core, i.e. its resistance to insertion of a peptide helix is neglected. The latter effect may be expected to modulate the timescale of changes in peptide/bilayer interactions observed in the simulations. One possible way in which to mimic this in our simplified model might be to damp the oscillations in peptide movements relative to the bilayer observed in our simulations.

The second approximation is the absence of explicit solvent molecules on either side of the bilayer phase. This is expected to effect electrostatic interactions between peptide sidechains. One possible way around this would be to divide the space into three dielectric regions, e.g.: (a) $\epsilon = 80$ for the aqueous phase; (b) $\epsilon = 10$ for the interfacial region; and (c) $\epsilon = 2$ for the bilayer core [36]. However, given the other approximations in our model such complexity is probably not justified.

The third approximation is that of a linear change in voltage across the bilayer. This ignores the surface potential of the bilayer due to a net charge on lipid headgroups, and also the surface dipole due to the carbonyl groups of the acyl chains [37]. However, most simulation studies to date have also employed a linear change in voltage [38–41]. In principle it would be possible to accommodate a more complex one-dimensional $V(z)$ function in the framework described in the Appendix.

4.2. Interpretation of results

The maps of the change in potential energy of a helix as it is rotated from a membrane associated to an inserted orientation fall into two classes. The first, exemplified by those for Ala_{20} and $\alpha 5$ provide clear evidence for an inserted orientation being favoured. The second class, as seen for $\alpha 7$, demonstrates that a membrane associated orientation is more favourable. The map for δ-toxin is somewhere between these two extremes, with an associated state favoured overall, but with an inserted state corresponding to a local energy minimum.

The results of the MD simulations reinforce and expand the predictions from energy mapping. For δ-toxin, the MD simulations show that a transbilayer voltage cannot drive insertion of the isolated helix, but that pre-existing inserted helices might become trapped in local energy minima. Experimentally, δ-toxin forms ion channels in a weakly voltage-dependent fashion. Such channels contain on average six helices per channel assembly [6]. Combined with the simulation results this suggests that channel formation does not proceed via voltage-driven insertion of isolated δ-toxin helices followed by pore assembly within the bilayer. Instead, some type of cooperative mechanism involving insertion of preformed assemblies of surface associated δ-toxin helices seems more likely [42].

The MD simulations for $\alpha 5$ and $\alpha 7$ reveal clear differences in their behaviour which nicely parallel those observed experimentally. Thus, in the simulations $\alpha 5$ undergoes voltage-induced insertion into a bilayer, whereas $\alpha 7$ clearly prefers a membrane associated location. Experimental studies of peptide/bilayer interactions [17] confirm this difference in preferred orientation between $\alpha 5$ and $\alpha 7$. Fur-

thermore, the $\alpha 5$ peptide forms transbilayer pores when added to lipid bilayers in the presence of a transbilayer voltage difference [43]. This correspondence between the simulation and experimental behaviour of $\alpha 5$ and $\alpha 7$ provides persuasive evidence that, despite the approximations, the simplified potential functions employed in these simulations provide useful information on peptide/bilayer interactions.

4.3. Biological relevance

From the simulations, one may suggest a plausible model for early insertion events of small α-helical peptides. This model may also be considered in the context of possible mechanisms for insertion of α-helical domains of integral membrane proteins [44]. In this model helices initially adopt a membrane-associated state and subsequently rotate into the bilayer so as to adopt a membrane-inserted state. Insertion is favoured by two terms: (a) E_{BIL}, reflecting the nature and position of the hydrophobic sidechains within the helix; and (b) $E_{\Delta V}$, dependent upon the size and sign of the transbilayer voltage difference, and on the position of charged sidechains within the helix. Our simulations also suggest that the conformation of the helices does not change markedly during the insertion process, i.e. to a first approximation they behave as rigid helical rods. Of course, this would be expected to be modulated by the presence of proline residues within helices. In this context, it will be of interest to simulate the peptide/bilayer interactions of alamethicin, a 20 residue peptide with a proline at position 14. There has been much speculation concerning the role of this proline as a molecular hinge during voltage-induced insertion of the alamethicin helix into a bilayer [45]. Current studies are directed towards extending our simulations to this and to more complex systems.

Acknowledgements

This work was supported by grants from the Wellcome Trust, and from the UK–Israel Science and Technology Research Fund. P.C. Biggin is an MRC research student. We wish to extend our thanks to Yechiel Shai (Weizmann Institute of Science) for his interest in this work, and the Oxford Centre for Molecular Science for computational facilities.

Appendix A. Smoothed transbilayer voltage function for use in MD simulations

In the absence of any smoothing, the transbilayer voltage component of the potential energy is given by:

$$E(z_j) = q_j \cdot V(z_j) = q_j \cdot \frac{\Delta V \cdot (z_j + d)}{2d} \qquad \text{(A1)}$$

where, for convenience, we have omitted Faraday's constant (see Eq. 4, above). Thus, given that the force (F) acting on a atom with charge q_j and the potential energy (E) of that atom are related by:

$$F = -\frac{\partial E}{\partial z};\ E = -\int_{-\infty}^{z} F \mathrm{d}z \qquad \text{(A2)}$$

if one can write an expression for the (smoothed) force then by integration one can obtain the (smoothed) energy. Without smoothing, the force is given by:

$$\begin{aligned} F &= 0 && \text{for } z \leftarrow d \\ F &= -q_j \cdot \frac{\Delta V}{2d} && \text{for } -d < z < +d \\ F &= 0 && \text{for } +d < z \end{aligned} \qquad \text{(A3)}$$

(noting that in the absence of smoothing the force is undefined for $z = \pm d$). By considering four regions of z, the function describing the force may be smoothed, giving:

$$\begin{aligned} F_1 &= \frac{A}{2}\exp\left(\frac{z+d}{\lambda}\right) && \text{for } z \leqslant -d \\ F_2 &= \frac{A}{2}\left[2 - \exp\left(\frac{-z-d}{\lambda}\right)\right] && \text{for } -d \leqslant z \leqslant 0 \\ F_3 &= \frac{A}{2}\left[2 - \exp\left(\frac{z-d}{\lambda}\right)\right] && \text{for } 0 \leqslant z \leqslant +d \\ F_4 &= \frac{A}{2}\exp\left(\frac{-z+d}{\lambda}\right) && \text{for } +d \leqslant z \end{aligned} \qquad \text{(A4)}$$

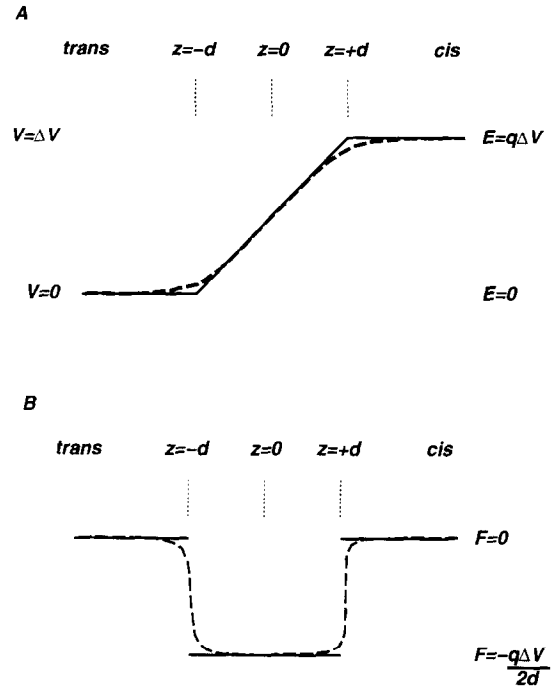

Fig. 7. Schematic diagram of (A) the potential energy due to the transbilayer voltage ($E_{\Delta V}$); and (B) the corresponding force (F). The diagram corresponds to a *cis* positive value of ΔV, and to a positive partial charge (q). The solid line indicates the unsmoothed energy (force) and the broken line the corresponding smoothed energy (force).

where $A = -q_j \cdot \Delta V/2d$ and where λ controls the extent of the smoothing. Typically, $\lambda = 2$ Å in our studies, with $d = 15$ Å. So, if the smoothed F is integrated one obtains the corresponding smoothed E:

$$E_1(z) = \int_{-\infty}^{z} F_1 \mathrm{d}z \qquad \text{for } z \leqslant -d$$

$$E_2(z) = E_1(-d) + \int_{-d}^{z} F_2 \mathrm{d}z \qquad \text{for } -d \leqslant z \leqslant 0$$

$$E_3(z) = E_2(0) + \int_{0}^{z} F_3 \mathrm{d}z \qquad \text{for } 0 \leqslant z \leqslant +d$$

$$E_4(z) = E_3(+d) + \int_{+d}^{z} F_4 \mathrm{d}z \qquad \text{for } +d \leqslant z \tag{A5}$$

Thus, both the force and the energy are defined for all values of z (Fig. 7).

References

[1] M.S.P. Sansom, Prog. Biophys. Mol. Biol., 55 (1991) 139.
[2] M.W. Parker and F. Pattus, TIBS, 18 (1993) 391.
[3] J. Li, Curr. Opin. Struct. Biol., 2 (1992) 545.
[4] M.S.P. Sansom, Nature Struct. Biol., 1 (1994) 563.
[5] J.E. Fitton, A. Dell and W.V. Shaw, FEBS Lett., 115 (1980) 209.
[6] I.R. Mellor, D.H. Thomas and M.S.P. Sansom, Biochim. Biophys. Acta, 942 (1988) 280.
[7] J.E. Alouf, J. Dufourcq, O. Siffert, E. Thiaudière and C. Geoffroy, Eur. J. Biochem., 183 (1989) 381.
[8] Y.P. Yianni, J.E. Fitton and C.G. Morgan, Biochem. Biophys. Acta, 856 (1986) 91.
[9] I.D. Kerr, J. Dufourcq, J.A. Rice, D.R. Fredkin and M.S.P. Sansom, Biochim. Biophys. Acta, 1236 (1995) 219.
[10] M.S.P. Sansom, I.D. Kerr and I.R. Mellor, Eur. Biophys. J., 20 (1991) 229.
[11] J. Schwartz et al., J. Membr. Biol., 132 (1993) 53.
[12] S.L. Slatin, A.C.K. and L. English, Biochem. Biophys. Res. Commun., 169 (1990) 765.
[13] J. Li, J. Carroll and D.J. Ellar, Nature, 353 (1991) 815.
[14] W. Ahmad and D.J. Ellar, FEMS Microbiol. Lett., 68 (1990) 97.
[15] D. Wu and A.I. Aronson, J. Biol. Chem., 267 (1992) 2311.
[16] E. Gazit, D. Bach, I.D. Kerr, M.S.P. Sansom, N. Chejanovsky and Y. Shai, Biochem. J., 304 (1994) 895.
[17] E. Gazit and Y. Shai, J. Biol. Chem., 270 (1995) 2571–2578.
[18] O. Edholm and F. Jähnig, Biophys. Chem., 30 (1988) 279.
[19] M. Milik, A. Kolinski and J. Skolnick, J. Phys. Chem., 96 (1992) 4015.
[20] J.L. Cornette, K.B. Cease, H. Margalit, J.L. Spouge, J.A. Berzovsky and C. DeLisi, J. Mol. Biol., 195 (1987) 659.
[21] M. Milik and J. Skolnick, Proteins: Struc. Func. Genet., 15 (1993) 10.
[22] M. Milik and J. Skolnick, Biophys. J., 69 (1995) 1382.
[23] M.A. Roseman, J. Mol. Biol., 200 (1988) 513.
[24] D.M. Engelman, T.A. Steitz and A. Goldman, Ann. Rev. Biophys. Biophys. Chem., 15 (1986) 321.
[25] I.D. Kerr, R. Sankararamakrishnan, O.S. Smart and M.S.P. Sansom, Biophys. J., 67 (1994) 1501.
[26] R. Sankararamakrishnan and M.S.P. Sansom, Biophys. Chem., 55 (1995) 215.
[27] J.P. Ryckaert, G. Ciccotti and H.J.C. Berendsen, J. Comput. Phys., 23 (1977) 327.
[28] H. Vogel, Biochem., 26 (1987) 4562.
[29] H.W. Huang and Y. Wu, Biophys. J., 60 (1991) 1079.
[30] S. Frey and L.K. Tamm, Biophys. J., 60 (1991) 922.
[31] E. Gazit and Y. Shai, Biochemistry, 32 (1993) 12363.
[32] K.H. Lee, J.E. Fitton and K. Wüthrich, Biochim. Biophys. Acta, 911 (1987) 144.
[33] M.J. Tappin, A. Pastore, R.S. Norton, J.H. Freer and I.D. Campbell, Biochemistry, 27 (1988) 1643.
[34] C.M. Bladon, P. Bladon and J.A. Parkinson, Biochem. Soc. Trans., 20 (1992) 862.
[35] C.M. Bladon, P. Bladon and J.A. Parkinson, J. Chem. Soc. Perkin Trans. 1, 109 (1993) 1687.

[36] A. Karshikoff, V. Spassov, S.W. Cowan and R.S.T. Landenstein, J. Mol. Biol., 240 (1994) 372.
[37] D.S. Cafiso, Curr. Opin. Struct. Biol., 1 (1991) 185.
[38] S.G. Galaktionov and G.R. Marshall, Biophys. J., 65 (1993) 608.
[39] B. Roux and M. Karplus, Biophys. J., 59 (1991) 961.
[40] A. Skerra and J. Brickmann, Biophys. J., 51 (1987) 977.
[41] K.S. Kim, J. Comp. Chem., 6 (1985) 256.
[42] G. Raghunathan, P. Seetharamulu, B.R. Brooks and H.R. Guy, Proteins: Struc. Func. Genet., 8 (1990) 213.
[43] E. Gazit and Y. Shai, Biochemistry, 32 (1993) 3429.
[44] G. von Heijne, Annu. Rev. Biophys. Biomol. Struct., 23 (1994) 167.
[45] M.S.P. Sansom, Eur. Biophys. J., 22 (1993) 105.